Preparation and characterization of ZnO nanorods grown into aligned TiO_2 nanotube array

S. Benkara [a,*], S. Zerkout [b]

[a] *Larbi Ben M'Hidi University, 04000 Oum El Bouaghi, Algeria.*
[b] *Ceramics laboratory, Mentouri University Constantine 25000, Algeria.*

Received in 01 Oct 2010, Revised 20 Nov, Accepted 21 Nov 2010.
Email: sali_benkara@yahoo.fr ; Tel.: +213 32 42 42; Fax: +213 32 42 41 26

Abstract

Nanocomposites of ZnO nanorods and TiO_2 nanotubes were fabricated via two steps: (1) Formation of TiO_2 nanotube arrays in HF solution by anodization method, (2) Deposition of ZnO nanorods by hydrothermal process with ammonia and Zinc nitrate as inorganic precursors. The morphological characteristics and structures of TiO_2 NTs and ZnO/TiO_2 NRs/Ts were examined by scanning electron microscopy (SEM), X-ray diffraction (XRD) and X-ray photoelectron spectroscopy (XPS). The diameter of the TiO_2 nanotube was approximately 60–95 nm. The ZnO nanoparticles are deposited on the top of TiO_2 nanotube or entered into tube. The anatase crystal of Titania and the hexagonal wurtzite crystal of zinc oxide forms were identified by XRD. The XPS analysis showed that the composite is made up of TiO_2 and ZnO.

Keywords: ZnO nanorods, TiO_2 nanotubes, Nanocomposites, Hydrothermal process, Anodic oxidation.

1. Introduction

Zinc oxide and Titanium dioxide have attracted considerable attention because of their great potential to solve environmental problems [1-3]. Among various nanoforms, one dimensional 1D nanostructures such as nanotubes and nanorods are considered to be one of the most important semiconductor nanomaterials for the expensive applications such as optics [4], electronics [5] mechanics [6], environmental [7-8], and biomedical-sensing [9] nanodevices.
Low degradation efficiency of TiO_2 nanofilms limited the application of the TiO_2 as photocatalyst [10]. It is an available way of the composite of nanofilms to improve the photocatalytic efficiency [11-15]. The nano ZnO/TiO_2 film would show higher photocatalytic efficiency than the efficiency of pure nano- ZnO film and nano- TiO_2 film. The photochemical performance was significantly enhanced on the ZnO/TiO_2 NRs/Ts electrode compared that pure TiO_2 NTs.
Unfortunately, the photocatalytic, photochemical, sensing, etc properties of this composite remain largely unexplored although a few studies focused on ZnO/TiO_2 nanocomposites [16-19].
Recently, various chemical, electrochemical, and physical deposition techniques have been utilized to fabricate ZnO/TiO_2 NR/Ts composite films.
Among these methods, template-assisted approach has been proven to be effective for the growth of ordered nanostructures [20-21]. Qiu et al [22-23] fabricated aligned TiO_2 nanotube arrays by using an aqueous solution synthesized ZnO nanorods as a template. Thitima et al also fabricate TiO_2 nanotubes using ZnO template [24].
Our strategy is to forme ZnO nanorod arrays from TiO_2 nanotubes. Since the widely used high temperature vapor-phase processes are expensive and energy consuming, the development of ZnO/TiO_2 films via chemical solution routes is widely desired [25], in particularly anodic oxidation [26-27] which is a simple technique to control the structure parameters of TiO_2 nanotube arrays as template and hydrothermal process to syntheses ZnO nanorods.
Effects of deposition conditions on the growth and orientation of ZnO/TiO_2 composite films were investigated and discussed in this paper.

2. Experimental

2.1 Materials and chemicals

Pieces of Titanium sheets (98% purity, 0.5 mm thickness), Zinc nitrate hexahydrite ($Zn(NO_3)_2.6H_2O$, AR), Hydrofluoric acid (HF), Acetone, Nitric acid HNO_3, Ammonia solution NH_4OH. Distilled water was used in all aqueous solution preparations and washing.

2.2 Preparation of TiO_2 nanotubes

Anodic oxidation method was adopted to prepare TiO_2 nanotubes TNTs. Prior to anodization, titanium pieces were degreased in an ultrasonic with distilled water for10 min, followed by eroding in a mixture of HF solution, nitric acid and distilled water for 1 min; then cleaned with acetone, rinsed with distilled water and dried in air. Anodization is performed in 2 w % HF solution and distilled water with voltage of 20 Volts for 5 h. Finally, samples were rinsed and annealed at 450 °C for 1 h.

2.3 Preparation of ZnO nanorods

ZnO nanorod arrays have been fabricated on TiO_2 nanotube substrate via hydrothermal process. The TiO_2 nanotube films was suspended in a sealed Teflon-lined autoclave with the volume of 50 ml, in which 40 ml of aqueous solution containing 0.02 M of $Zn(NO_3)_2.6H_2O$ and (0.3-0.4) M of NH_3H_2O, followed by heating at 80°C-100 °C-160 °C for 24h. At last the products were thoroughly washed and dried in air.

2.4 Characterization of resulting films samples

The surface morphology of the film samples was observed through scanning electron microscopy (SEM-JEOLJSM-7600 and LE0438vp apparatus). The crystal phase composition of the samples were analyzed by X-ray diffraction (XRD, Bruker-Siemens D8- Advance, Cu.Kα radiation λ=1.5406 A°), and by X-ray photoelectron spectroscopy XPS.

3. Results and discussion

Fig.1 is the profiles of the TiO_2 nanotubes before and after annealing at 450 C° for 1 h.

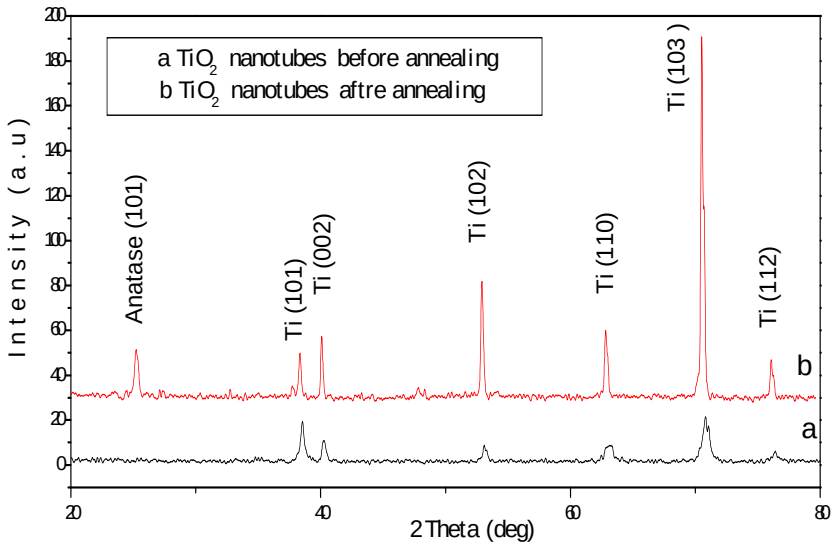

Fig.1 The XRD patterns of TiO_2 NTs before annealing (a) and after annealing (b).

As shown in fig.1.b, peaks with 2θ value of 25.6° correspond to the crystal plan of anatase (101) phase. And other peaks are corresponding to the titanium substrate, which is similar to the results found in many literatures [28] and [19].

Fig.2 presents XRD patterns of ZnO/TiO_2 at different temperatures. Except for the peaks of titanium and titania, the diffraction peaks with 2θ value of: 32.1°, 34.7° and 36.5° agree well with the wurtzite hexagonal structure with the lattice constants of: a=0.32 nm and c= 0.52 nm according to the standard JCPDS card (No. 36-1451). Based on the higher (002) XRD peak than (101) one, which is usually the highest in all XRD peaks of ZnO crystal.

XRD patterns in Fig.2.c show a disappearance of the peaks corresponding to titanium, at high temperature, the formation of ZnO increases with increasing of reaction rate into aqueous solution, and also the reaction rate between Ti and ZnO.
No remarkable change in orientation of the films as the amount of ammonia was increased shown in Fig.3 but influenced the intensity of the preferred crystalline orientation.

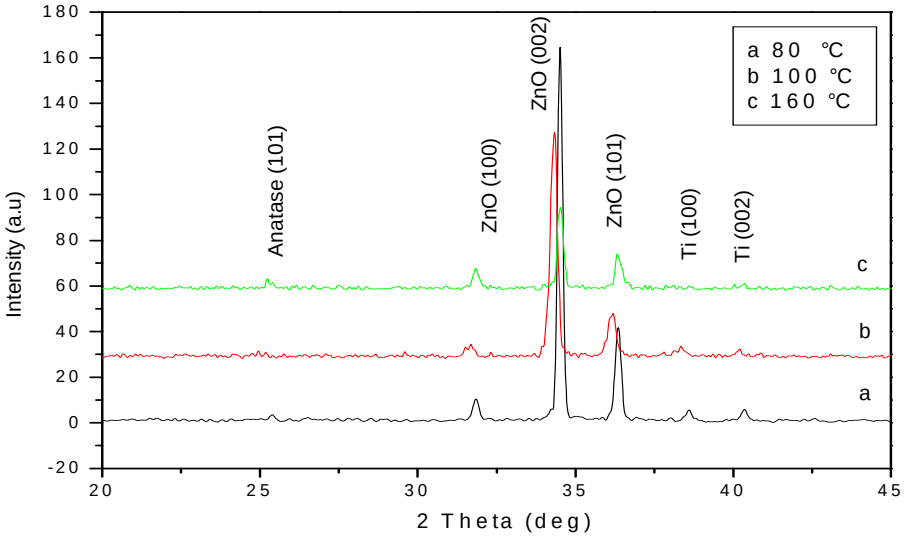

Fig. 2. The XRD patterns of ZnO/TiO2 at different hydrothermal temperature: at 80 °C (a), at 100 °C (b) and at 160 °C (c).

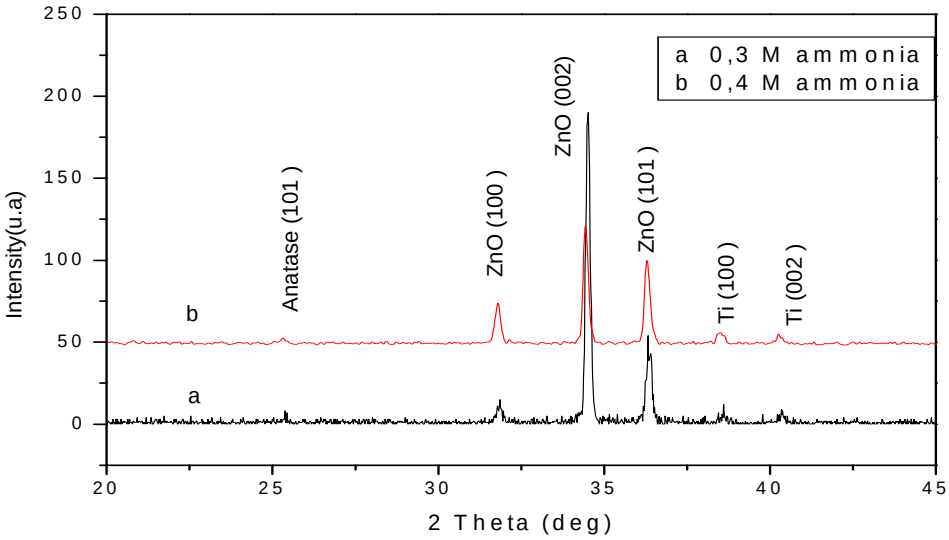

Fig. 3 The XRD patterns of ZnO/TiO2 with 0,3 M (a) and 0,4 M of ammonia (b).

The SEM image of the TiO_2 nanotubes formed on the Ti substrate by anodization method shown in Fig.4.a, which reveals that high density, well ordered and uniform nanotubes array are formed. The diameters of these nanotubes range from 60 nm to 95 nm and their length is about 1.7 µm detected by pofilometry.
After ZnO deposition by hydrothermal process on the TiO_2 NTs as shown in Fig.4.b, the ZnO grows oriented through the TiO_2 NTs inner channels. The epitaxial growths of ZnO nanorods inside the TiO_2 nanotube channels are spilled over the TiO_2, which is in good agreement with one reported by Z. Zhang et al [19] and K. Yu et al [29].
XSP measurements were performed to determine the chemical composition of the prepared films and the valence states of various species. Fig.5 shows the XPS survey spectra of ZnO/TiO_2 nanotube composite. The peaks appear in specter are mainly attributed to Ti, O, Zn and C element. A C1s peak observed in survey spectra comes from

widespread presence of carbon in the environment. The high resolution XPS spectra in Fig.5 (b-d) show the characteristic peaks of Ti 2p, Zn 2p and O1s, respectively of ZnO/TiO_2.
The peaks located at 459.6 and 465.4 eV are attributed to Ti 2p components, which are in good agreement with the titanium (IV) species. The binding energy peak located at 1021.3 eV is attributed to the Zn 2p. It means that Zn ions are in form of ZnO. As seen in Fig.5.d the peak of O1s is deconvoluted by using symmetric Gaussian curves resulting in a peak at 529.6 eV relates to the oxygen atoms of TiO_2, a peak at 531,1 eV relates to the oxygen atoms of ZnO, and the peak of 533.04 eV related to the oxygen atoms of H_2O.

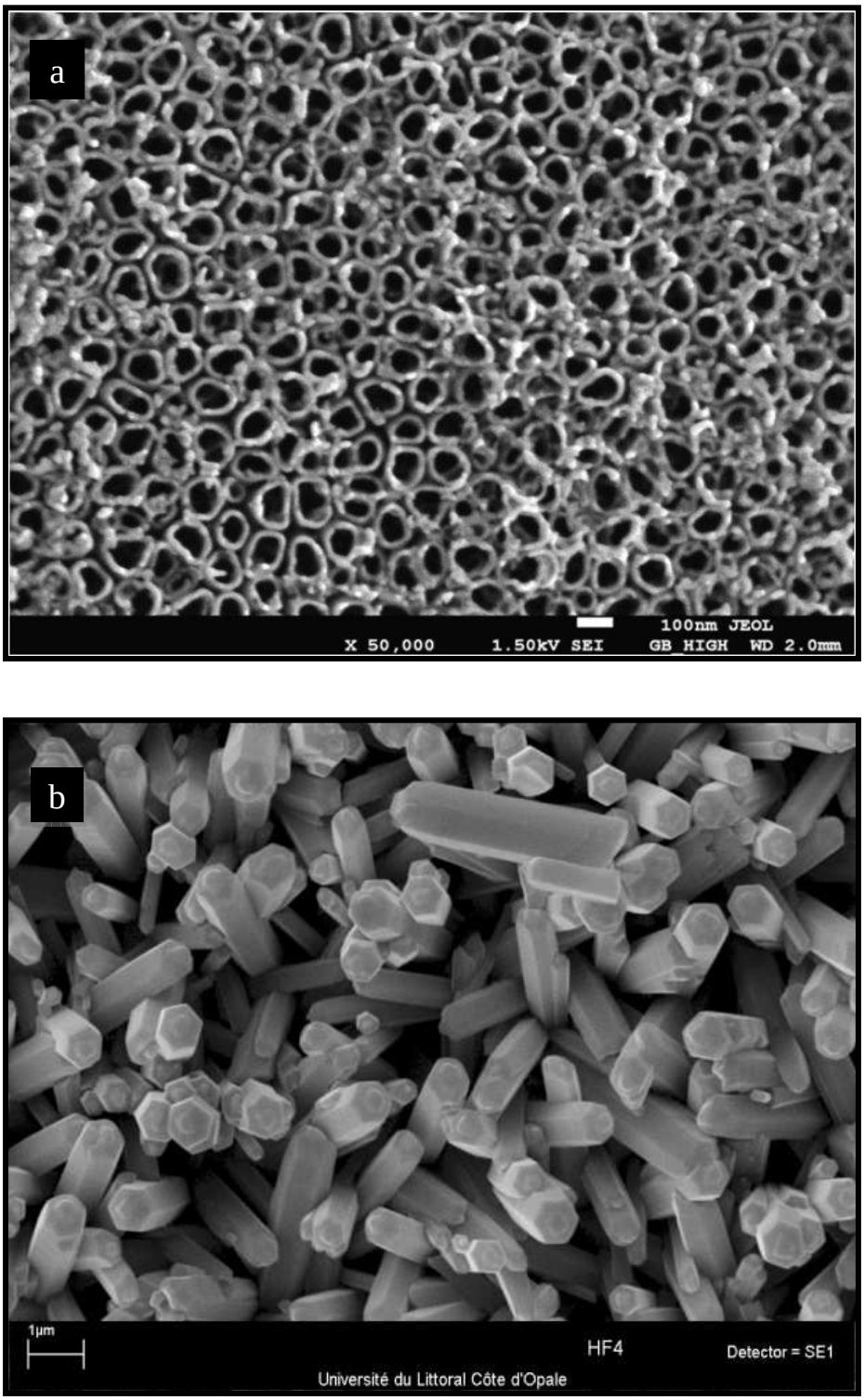

Fig. 4. SEM images of TiO_2 nanotube (a) and ZnO/TiO_2 nanocomposite (b)

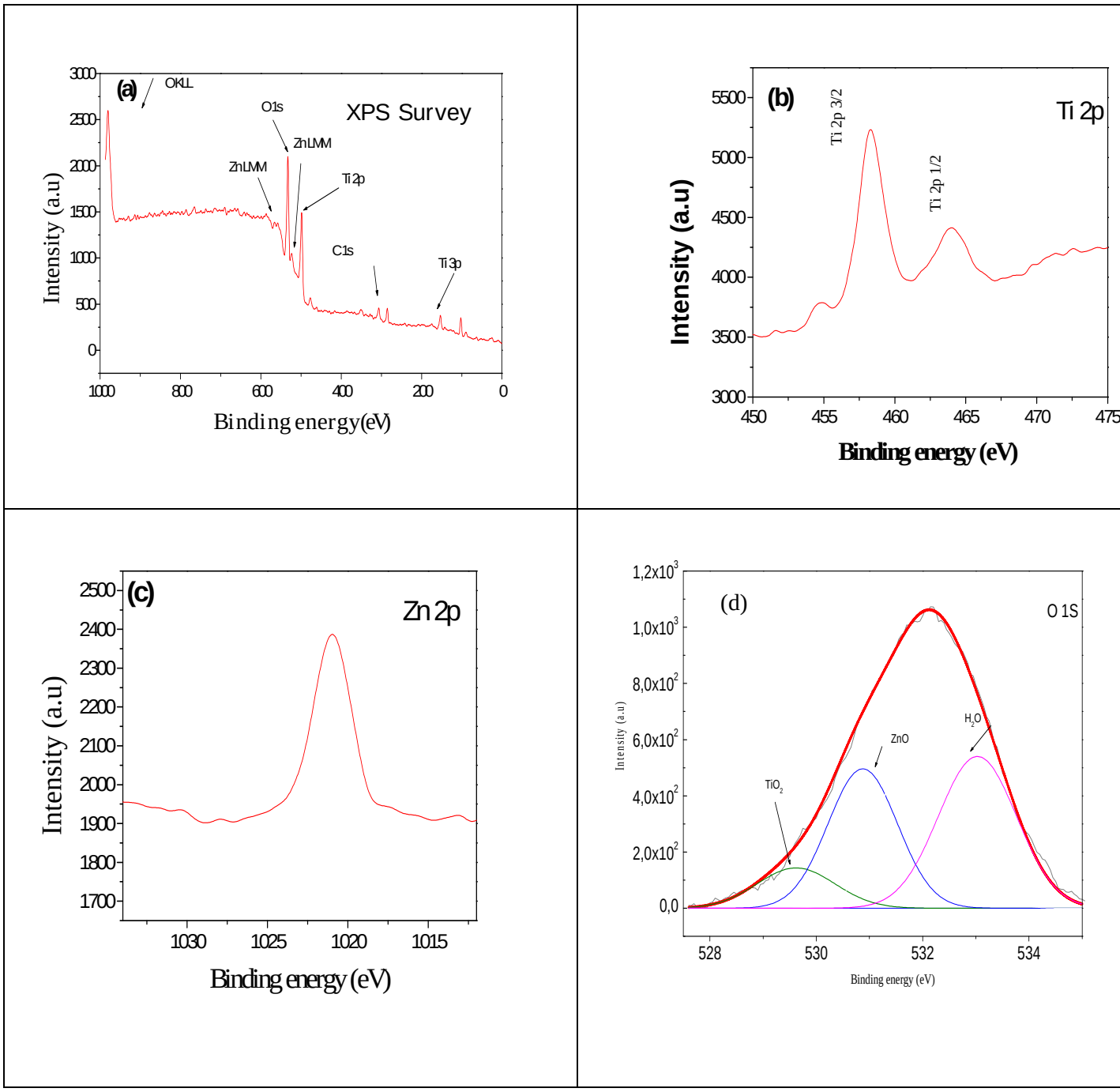

Fig. 5. (a) XPS survey spectra of ZnO/TiO_2 nanocomposite, (b) Ti 2p XPS spectra, (c) O 1s XPS spectra, (d) Zn 2p XPS spectra.

4. Conclusion

ZnO/titanate nanocomposites were fabricated via two step route. The TiO_2 nanotubes were fabricated by anodization method. The hydrothermal process was employed to form ZnO nanorods into TiO_2 nanotubes. The obtained TiO_2 nanotubes and ZnO/TiO_2 nanocomposite are characterized by different techniques: XRD, SEM and XPS. TiO_2 nanotubes are mainly anatase structure and well ordered. The diameter of these nanotubes ranges from 60 to 95 nm and the length is about 1.7 µm. The ZnO nanorods have high crystallinity of wurtzite hexagonal structure.

References

1. Pan, Z.W., Dai, Z.R., Wang, Z.L., *Science* 291 (2001) 1947.
2. Wu, J.J., Tseng, C.H., *Appl. Catal.* B 66 (2006) 51.
3. Wang, Y.W., Zhang, L.Z., Deng, K.J., Chen, X.Y., Zou, Z.G. *J. Phys. Chem. C* 111 (2007) 2709.
4. Zamfirescu, M., A. Kavokin, B. Gil, G. Malpuech, M. Kaliteevski, *Phys. Rev. B* 65 (2002), 161205(1–4).
5. Bavykin, D.V., A.A. Lapkin, P.K. Plucinski, L.T. Murciano, J.M. Friedrich, F.C.Walsh, *Top. Catal.* 39 (2006) 151.
6. Zhonglin Wang, Jinhui Song, *Science* 312 (2006) 242.
7. Mor GK, Carvalho MA, Varghese OK, Pishko MV, Grimes CA. *J. Mater. Res.* 19 (2004) 628.
8. Paulose M, Varghese OK, Mor GK, Grimes CA, Ong KG, *Nanotechnology* 17 (2006) 398.
9. Wan, Q., Q.H. Li, Y.L. Chen, T.H. Wang, X.L. He, J.P. Li, *Appl. Phys. Lett.* 84 (2004) 3654.
10. Zhang, Z., Y.Yuan, Y.Fang, L.Liang, *Talanta* 73 (2007) 523.
11. Noorjahan, M., V.D. Kumari, M. Subrahmanyam, P. Boule, *Appl. Catal.* B 47 (2004) 209.
12. Dhananjeyan, M.R., E. Mielczarski, K.R. Thampi, P. Buffat, M. Bensimon, A. Kulik, J. Mielczarski, J. Iwi, *J. Phys. Chem. B* 105 (2001) 12046.
13. Takeuchi, M., S. Dohshi, T. Eura, M. Anpo, *J. Phys. Chem.* B 107 (2003) 14278.
14. Marci, G., V. Augugliaro, M.J. Lopez-Munoz, C. Martin, L. Palmisano, V. Rives, M. Schiavello, R.J.D. Tilley, A.M. Venezia, *J. Phys. Chem.* B 105 (2001) 1026.
15. Mane, R.S.,W.J. Lee, H.M. Pathan, S.H. Han, *J. Phys. Chem. B* 109 (2005) 24254.
16. Yang, S.G., X. Quan, X.Y. Li, Y.Z. Liu, S. Chen, G.H. Chen, *Phys. Chem. Chem. Phys.* 6 (2004) 659.
17. Yoon, K.H., J. Cho, D.H. Kang, *Mater. Res. Bull.* 34 (1999) 1451.
18. Ohshima, K., K. Tsuto, K. Okuyama, N. Tohge, *Aerosol Sci. Technol.* 19 (1993) 468.
19. Zhang, Z., Y. Yuan, L. Liang, Y. Cheng, *Journal of Hazardous Materials* 158 (2008) 517.
20. Lee S, Jeon C, Park Y (2004) *Chem. Mater.* 16:4292.
21. Park I, Jang S, Hong J, Vittal R, Kim K., *Chem. Mater*. 15 (2003) 4633.
22. Qiu, J., Z. Jin, Z. Liu, X. Liu, G. Liu,W.Wu, X. Zhang, X. Gao, *Thin Solid Films* 515 (2007) 2897.
23. Qiu, J., W. Yu, X. Gao, X. Li, *Nanotechnology* 17 (2006) 4695.
24. Thitima. R, Takashi. S, Susumu.Y. *Solar Energy Materials & Solar Cells* 92 (2008) 1445.
25. Shr-Nan Bai, Tseung-Yuen Tseng. *J Mater Sci: Mater Electron*, 20 (2009) 604.
26. Gong, D., C.A. Grimes, O.K. Varghese, Z. Chen, W. Hu, E.C. Dickey, *J. Mater. Res.* 16 (2001) 3331.
27. Xie, Q., S.G. Yang, X.L. Ruan, H.M. Zhao, *Environ. Sci. Technol.* 39. (2005) 3770.
28. Chen, J.B., C.W. Wang, B. H. Ma, Y. Li, J. Wang, *Thin Solid Films*, 517 (2009) 4390.
29. Yu, K., Z. Jin, X. Liu, J. Zhao, J. Feng, *Applied Surface Science* 253 (2007) 4072.